Boron-Doped Diamond Microelectrodes Reveal Reduced Serotonin Uptake Rates in Lymphocytes from Adult Rhesus Monkeys Carrying the Short Allele of the *5-HTTLPR*

Yogesh S. Singh,[†] Lauren E. Sawarynski,[‡] Heather M. Michael,[⊥] Robert E. Ferrell,[#] Michael A. Murphey-Corb,[⊥] Greg M. Swain,[▽] Bhavik A. Patel,[○] and Anne M. Andrews*[,†,§,∥,◆]

[†]Departments of Chemistry, and [‡]Bioengineering, and [§]Veterinary and Biomedical Sciences, and [∥]Huck Institutes of Life Sciences, Pennsylvania State University, University Park, Pennsylvania 16802, [⊥]Department of Microbiology and Molecular Genetics, and [#]Department of Human Genetics, University of Pittsburgh School of Medicine, Pittsburgh, Pennsylvania 15261, [▽]Department of Chemistry, Michigan State University, East Lansing, Michigan 48824, [○]Department of Bioengineering, Imperial College London, London, U.K. SE7 2AZ, and [◆]Department of Psychiatry & Biobehavioral Sciences and California NanoSystems Institute, University of California, Los Angeles, California 90024

Abstract

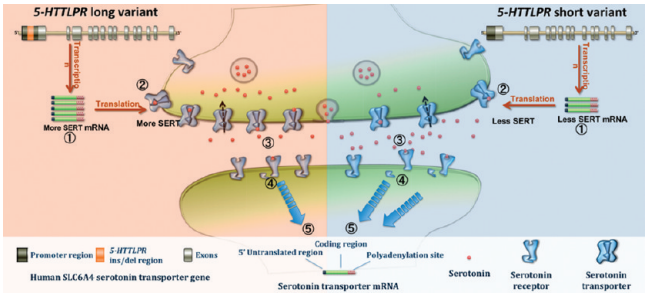

Uptake resolved by high-speed chronoamperometry on a second-by-second basis has revealed important differences in brain serotonin transporter function associated with genetic variability. Here, we use chronoamperometry to investigate variations in serotonin transport in primary lymphocytes associated with the rhesus serotonin transporter gene-linked polymorphism (*rh5-HTTLPR*), a promoter polymorphism whose orthologues occur only in higher order primates including humans. Serotonin clearance by lymphocytes is Na^+-dependent and inhibited by the serotonin-selective reuptake inhibitor paroxetine (Paxil), indicative of active uptake by serotonin transporters. Moreover, reductions in serotonin uptake rates are evident in lymphocytes from monkeys with one or two copies of the short '*s*' allele of the *rh5-HTTLPR* ($s/s < s/l < l/l$). These findings illustrate that *rh5-HTTLPR*-related alterations in serotonin uptake are present during adulthood in peripheral blood cells natively expressing serotonin transporters. Moreover, they suggest that lymphocytes can be used as peripheral biomarkers for investigating genetic or pharmacologic alterations in serotonin transporter function. Use of boron-doped diamond microelectrodes for measuring serotonin uptake, in contrast to carbon fiber microelectrodes used previously in the brain, enabled these high-sensitivity and high-resolution measurements. Boron-doped diamond microelectrodes show excellent signal-to-noise and signal-to-background ratios due mainly to low background currents and are highly resistant to fouling when exposed to lymphocytes or high concentrations of serotonin.

Keywords: Serotonin transporter, promoter polymorphism, nonhuman primate, peripheral blood mononuclear cells, chronoamperometry, voltammetry, carbon fiber microelectrode

Microelectrode voltammetry, which comprises a group of related electrochemical techniques, is a rapidly growing means to explore chemical neurotransmission (*1*). The expanding use of voltammetry for neurochemical studies is largely due to advantages associated with the ability to perform *in situ* measurements with excellent spatial and temporal resolution. Moreover, strategies for parlaying electrochemical detection of nonelectroactive neurotransmitters have been devised (*2*, *3*). The benefits of making direct measurements in tissue are highly evident in recent work using high-speed chronoamperometry to investigate changes in serotonin uptake rates associated with decreases in serotonin transporter (SERT) gene expression. Reduced brain serotonin uptake associated with the loss of one functional copy of the SERT gene in mice is readily observed using chronoamperometry *ex vivo* (*4*) and *in vivo* (*5*). By contrast, these changes are not differentiable using standard radiochemical

Received Date: August 29, 2009
Accepted Date: October 24, 2009
Published on Web Date: November 16, 2009

DOI: 10.1021/cn900012y | *ACS Chem. Neurosci.* (2010), *1*, 49–64

methods (*6*, *7*). Furthermore, maximal uptake rates appear to be underestimated, while the affinity of serotonin for its transporter is overestimated using traditional [^{3}H]-serotonin uptake. We have attributed this to a loss of transported serotonin occurring during the filtration process employed in radiometric methods (*6*). The radiochemical assay also suffers from shortcomings associated with estimating uptake rates using a single time point, in contrast to chronoamperometry and other voltammetry methods, which provide information on neurotransmitter transport over the entire time course with second to millisecond resolution.

Carbon fiber microelectrodes (CFMs) have most often been used for voltammetry measurements of neurotransmitters (*8*). Advantages associated with this type of microelectrode include the commercial availability of carbon fibers with diameters ranging from 3 to 30 μm and the ease of fabrication of small cylindrical or disk-shaped microelectrodes providing spatially resolved measurements in the brain (*9*). Despite these advantages, CFMs have limitations associated with sp^2-hybridized carbon and the presence of surface hydroxyl groups, both of which promote strong adsorption of polar analytes via dipole−dipole, ion−dipole, and hydrogen bonding interactions (*10*−*13*). Additional problems arise when using CFMs to detect serotonin, which forms an unstable oxidation byproduct that can dimerize (*14*, *15*). These products adhere to CFM surfaces causing electrode fouling (*16*). Thus, CFMs are not ideal for measurements of serotonin at concentrations greater than 1 μM (*17*) or for longer exposures to biological preparations.

Boron-doped diamond is a highly stable sp^3-hybridized form of carbon that lacks an extended π-electron system and whose surface is dominated by hydrogen-termination (*18*−*22*). Together, these characteristics impart electrodes fabricated from boron-doped diamond with a nonpolar surface chemistry making them more resistant to fouling (*23*). Serotonin release by enterochromaffin cells in the intestinal mucosa, where tissue serotonin concentrations are estimated to be in the micromolar range (*24*), has been measured using boron-doped diamond microelectrodes (BDMs) and constant potential amperometry (*23*, *25*). Here differences in uptake associated with lower levels of SERT expression in neonatal intestinal mucosa were differentiated from those in adult gut tissue (*26*).

The serotonin transporter is a major research focus because of its primary role in regulating the neuromodulatory effects of serotonin in the central and peripheral nervous systems (*27*, *28*). The SERT is the primary molecular target for the serotonin-selective reuptake inhibitors (SSRIs), which are commonly prescribed drugs used in the treatment of depression and anxiety disorders. Widely abused drugs, including 3,4-methylenedioxymethamphetamine (MDMA; Ecstasy) and cocaine, also have primary mechanisms of action at the SERT (*7*, *29*, *30*).

Beyond its pharmacologic significance, a number of commonly occurring polymorphisms have been discovered in the noncoding regions of the human SERT gene (*31*−*35*). Additionally, rare coding region single nucleotide polymorphisms (SNPs) have been pinpointed (*36*), some of which are of psychiatric relevance (*35*, *37*, *38*). A 43-base pair insertion/deletion promoter polymorphism, termed the human serotonin transporter gene-linked polymorphic region (*h5-HTTLPR*), is the most extensively studied SERT gene variant (Figure 1) (*31*). This polymorphism has been linked to differences in anxiety-related personality traits, vulnerability to developing neuropsychiatric disorders, and variability in drug responsiveness (*28*, *31*, *39*−*41*). The *h5-HTTLPR* is hypothesized to influence brain function and behavior via allele-specific SERT promoter activity (*42*, *43*). Decreases in SERT mRNA (*31*) and protein binding in postmortem human brain (*44*) have been associated with the lower expressing short '*s*' allele. However, not all studies are in agreement. For example, SERT mRNA levels in human postmortem raphe tissue (*45*) and *in vivo* human SERT binding measured by positron emission tomography (PET) (*46*) have failed to show *h5-HTTLPR*-associated allele specific differences.

Rhesus monkeys (*M. mulatta*) express a serotonin transporter gene-linked polymorphic region, the *rh5-HTTLPR*, which is evolutionarily related to the *h5-HTTLPR* (*47*, *48*). The *rh5-HTTLPR* is a 21 base pair insertion/deletion promoter polymorphism that occurs at a locus slightly shifted from that in humans. Serotonin transmission, stress responsiveness, and social behavior are influenced by the *rh5-HTTLPR* (*49*−*52*), similar to associations between the *h5-HTTLPR* and human behavior. At the molecular level, the *rh5-HTTLPR* is also hypothesized to affect transcription of SERT. However, its influence on SERT mRNA, protein levels, and serotonin uptake has not been determined, and only its effects in a reporter gene assay have been described (*53*).

The close parallels between the *h5-HTTLPR* and *rh5-HTTLPR* provide opportunities to use the latter to advantage for investigating this evolutionarily conserved polymorphism, which is absent in lower order mammals including rodents (*47*). For example, the *h5-HTTLPR* possesses additional functional promoter region SNPs (*32*−*34*), multiplying the number of genotypes and complicating their interpretation (*54*). By contrast, orthologous SNPs have not been reported in the *rh5-HTTLPR*. Furthermore, establishing the relationship between the effects of the *rh5-HTTLPR* in peripheral tissues vs the brain is possible. By contrast, with the exception of *in vivo* imaging techniques, which currently

DOI: 10.1021/cn900012y | *ACS Chem. Neurosci.* (2010), *1*, 49–64

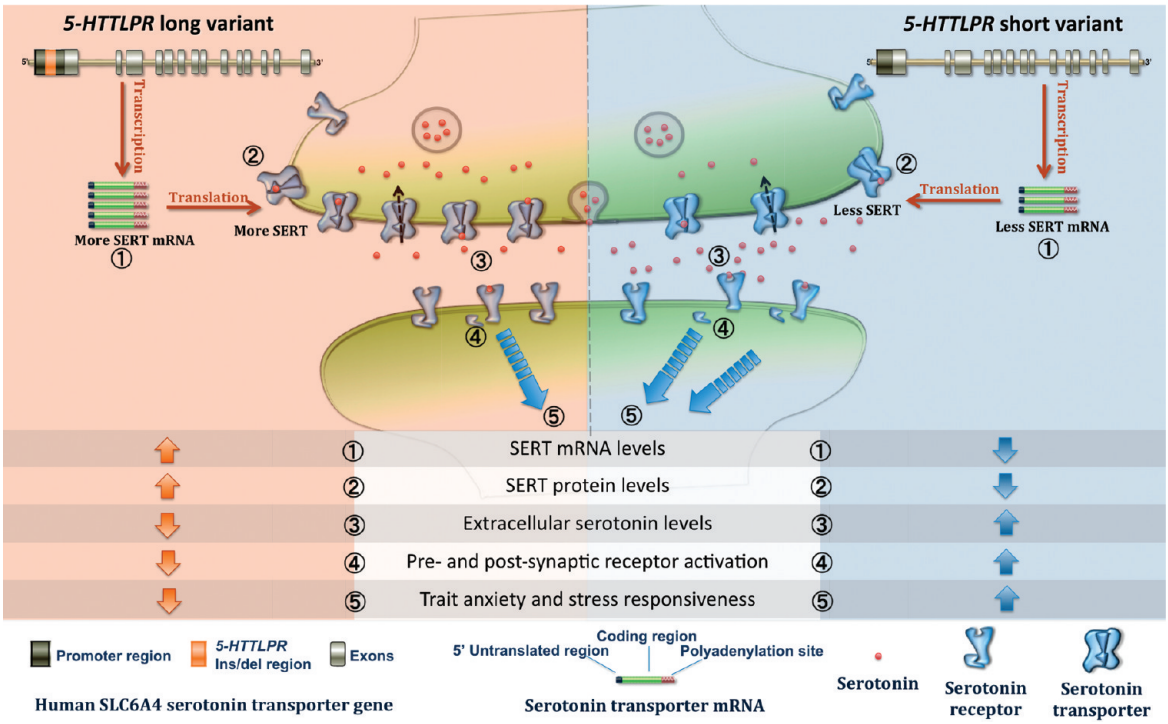

Figure 1. Proposed effects of the *5-HTTLPR* on the serotonergic system and behavior. The serotonin transporter gene-linked polymorphic region (*5-HTTLPR*) is a promoter polymorphism that occurs only in higher order primates, including humans and rhesus monkeys. In human subpopulations, the short '*s*' allele has been observed at frequencies of 25%, 40%, or 80% in African Americans, European Americans, or Japanese, respectively (*97*). The frequency of the orthologous '*s*' allele in rhesus monkeys is ~25% (*48*). In both species, the short form of the *5-HTTLPR* is hypothesized to lower transcription rates compared to the long '*l*' form, resulting in decreased SERT mRNA, lower SERT protein levels, and, hence, reduced serotonin uptake and increased extracellular serotonin levels (*28*, *84*). However, while the molecular and neurochemical effects of the *5-HTTLPR*, including its influence during different times in the life cycle and the elucidation of critical downstream targets, are still under investigation, many studies have found significant associations between the *5-HTTLPR* short allele and higher trait-anxiety or increased stress responsiveness in humans and rhesus monkeys (for recent reviews see refs (*28*, *40*, and *54*). This is in contrast to the effects of chronic treatment with serotonin reuptake inhibiting antidepressants in adults, which are also hypothesized to increase extracellular serotonin, but which produce decreased anxiety and/or elevated mood in the subset of patients clinically responsive to these medications.

have low resolution, making these types of connections in living humans are difficult.

Here, we take a key step toward understanding the effects of the *rh5-HTTLPR* on SERT function. We employ high-speed chronoamperometry to explore serotonin uptake in nontransformed primary rhesus lymphocytes, which natively express low levels of SERT. We investigate whether BDMs have advantages over CFMs for measuring serotonin uptake in these cells. Furthermore, we test the hypothesis that *rh5-HTTLPR* genotype is associated with variations in serotonin uptake rates in adult animals. On the basis of our findings, we anticipate that readily obtainable peripheral blood lymphocytes, in combination with sensitive electrochemical methods, will provide opportunities for future studies aimed at understanding the effects of gene variants, neurological disease states, and drug treatment on SERT function.

Results and Discussion

Electrode Responses to Serotonin

Cyclic voltammetry was used to compare background and serotonin-related currents at BDMs vs CFMs. Figure 2 depicts representative cyclic voltammetric *i-E* curves obtained at 1 V/s in assay buffer (background) or 10 μM serotonin. Boron-doped diamond microelectrodes exhibited 6-fold lower background currents on average compared to those of CFMs, even though the surface areas of BDMs (~30,000 μm^2) were larger than CFM surface areas (~11,000 μm^2). Lower background currents at BDMs have been attributed to the absence of redox-active or ionizable surface groups (reduced pseudocapacitance) and slightly lower concentrations of internal charge carriers (reduced capacitance) (*19*). The mean oxidation to background current ratio produced by 10 μM serotonin at BDMs (0.58 ± 0.03) was significantly higher than that at CFMs (0.13 ± 0.03; $P < 0.0001$).

For serotonin, the half-wave oxidation potential ($E_{1/2}^{ox}$) at BDMs (0.54 ± 0.008 V) was significantly greater than that at CFMs (0.32 ± 0.005 V; $P < 0.0001$). Oxidation of monoamine neurotransmitters proceeds via an inner-sphere electron transfer pathway; thus, electron transport kinetics are highly sensitive to electrode surface characteristics (*18*, *19*). Adsorption of serotonin on

DOI: 10.1021/cn900012y | ACS Chem. Neurosci. (2010), 1, 49–64

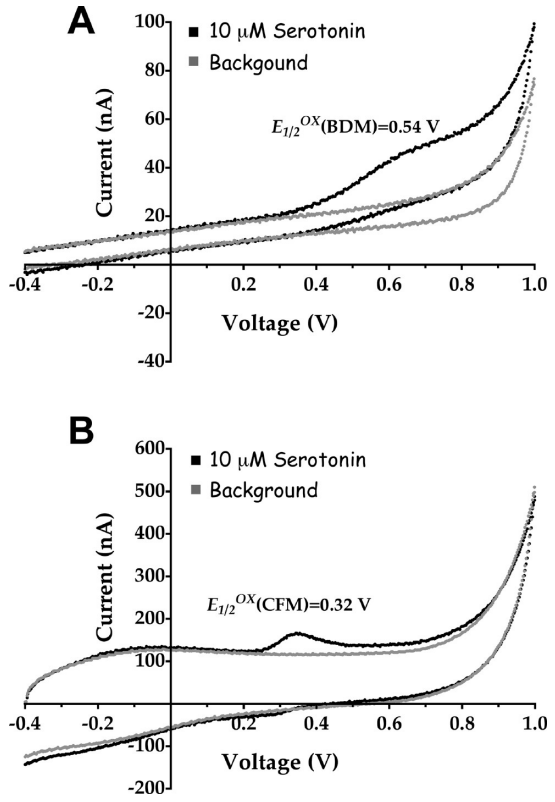

Figure 2. Cyclic voltammetry comparing background and serotonin-related currents. Representative slow scans before and after the introduction of 10 μM serotonin at (A) a 70 μm cylindrical boron-doped diamond microelectrode (BDM) and (B) a 30 μm cylindrical carbon-fiber microelectrode (CFM). Each scan represents the average of 10 consecutive scans. Potentials were scanned from −0.4 to 1 V and back to −0.4 V at a rate of 1 V/s. The average serotonin oxidation half-wave potential ($E_{1/2}^{ox}$) at BDMs (0.5 ± 0.008 V; N = 4 electrodes) was significantly higher than that at CFMs (0.3 ± 0.005 V; N = 5 electrodes) [$t(7)$ = 24, P < 0.0001]. Moreover, the signal-to-background ratio produced by 10 μM serotonin at BDMs (0.58 ± 0.03) was significantly higher than at CFMs (0.13 ± 0.03; [$t(7)$ = 11, P < 0.0001]) resulting from decreased background currents [$t(7)$ = 3.9, P < 0.01] at BDMs.

electrode surfaces facilitates charge transfer leading to an increase in the heterogeneous electron transfer rate constant and faster kinetics. A positive shift in the oxidation potential for serotonin at BDMs vs CFMs has been hypothesized to be due to slower reaction kinetics resulting from lower adsorption of serotonin at BDM surfaces. Similar increases in $E_{1/2}^{ox}$ at BDMs compared to CFMs have also been reported for norepinephrine (*55*).

These cyclic voltammetry data suggested that oxidation potentials higher than those typically used with CFMs would be needed to produce maximal serotonin currents when employing BDMs in combination with chronoamperometry. To investigate this, integrated currents produced by 1 μM serotonin at different oxidative step potentials were evaluated, while the reductive and resting potentials were held constant at 0 V. Varying E^{ox} from 0.3 to 0.7 V in 0.1 V increments produced significant increases in integrated current that reached a plateau at 0.8 V (P < 0.01 for steps below 0.8 V vs 0.8 V), after which no significant increases in integrated current were observed (P > 0.05 for steps above 0.8 V vs 0.8 V) (Figure 3A). Increasing E^{ox} to values higher than 0.8 V resulted in significant decreases in signal-to-noise ratios (P < 0.01 for 1 V vs 0.8 V) and signal-to-background ratios (P < 0.01 for 0.9−1 V vs 0.8 V) (Figure 3A) mainly attributable to increases in noise and background currents, respectively. Together, these results suggest that an E^{ox} of 0.8 V produces the highest integrated oxidation current while also maximizing signal-to-noise and signal-to-background ratios for detecting serotonin at BDMs by chronoamperometry.

Next, we compared the responses of BDMs vs bare CFMs to serotonin concentrations ranging from 0.5 to 10 μM (Figure 3B). Boron-doped diamond microelectrodes showed highly linear responses over the entire concentration range investigated (R^2 = 0.9908). By comparison, CFMs showed lower linearity (R^2 = 0.9579) with a better fit to a nonlinear curve (one-site exponential, R^2 = 0.9789). Analysis of the electrode responses at each serotonin concentration showed significantly lower responses of CFMs compared to BDMs (P < 0.01) at 2.5 μM and higher, probably due to fouling of CFM surfaces.

Carbon fiber microelectrodes have been used extensively for *in vivo* and *ex vivo* detection of neurotransmitters, and application of Nafion to CFMs has been shown to increase neurotransmitter current, signal-to-background ratios, and limits of detection (*56*−*58*). Boron-doped diamond, which is still in its early stages for use in monoamine neurotransmitter sensing, has been compared to glassy carbon (*20*, *59*) or bare CFMs (*23*). Here, we contrasted BDMs with both bare and Nafion-coated CFMs for measuring serotonin using chronoamperometry by assessing four key electrode properties: signal (nC/mm^2), signal-to-noise, signal-to-background (%), and limits of detection (nM) (Table 1). With the exception of the signal itself, which was only modestly higher at BDMs vs bare CFMs (P < 0.05), BDMs showed highly improved figures of merit (P < 0.001 vs CFMs and Nafion-coated CFMs), further indicating that boron-doped diamond is a superior electrode material for serotonin sensing compared to carbon fiber primarily based on lower background currents and noise.

Boron-Doped Diamond Microelectrodes Show Reduced Fouling

Carbon-fiber electrode surfaces show adsorption of polar analytes such as serotonin and its oxidation products (*14*, *15*). Furthermore, biological macromolecules adsorb to CFM surfaces, and both of these processes cause fouling, thus altering time-dependent amperometric responses to analytes (*60*, *61*). Commonly used techniques to reduce CFM fouling involve coating

DOI: 10.1021/cn900012y | ACS Chem. Neurosci. (2010), 1, 49–64

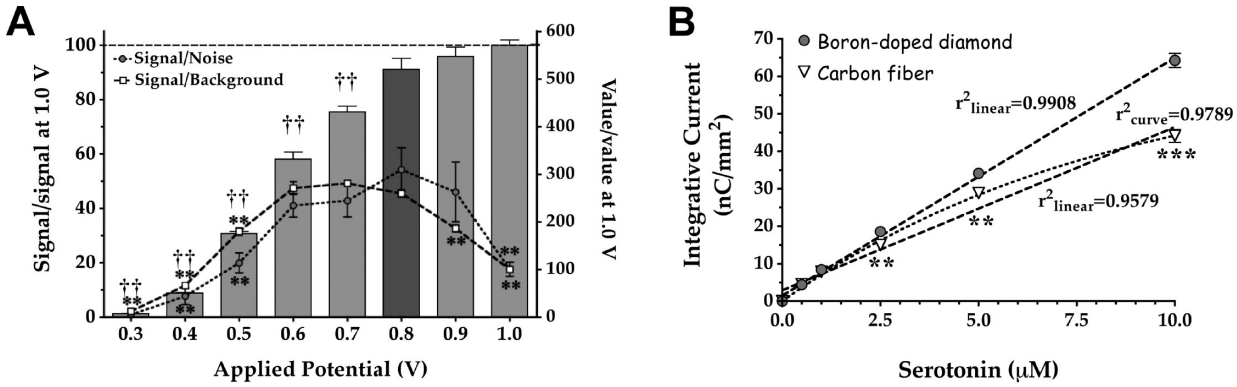

Figure 3. Potential and current responses to serotonin at BDMs by chronoamperometry. (A) The effects of varying the applied potential (E^{ox} = 0.3−1.0 V) on integrated current produced by 1 μM serotonin at boron-doped diamond microelectrodes (BDMs) was evaluated using chronoamperometry while maintaining constant reductive and resting potentials at 0 V. Bars represent the ratios of mean integrated current recorded at each applied potential with respect to the mean value at 1.0 V (left *y*-axis). Varying the applied potential had a statistically significant effect on integrative current [$F(7,24) = 360$, $P < 0.0001$]. Specifically, increasing the applied potential between 0.3 and 0.8 V resulted in significant increases in integrative oxidation current ($P < 0.001$ for each potential step below 0.8 V vs 0.8 V), while increasing E^{ox} further failed to produce additional increases in current ($P > 0.05$ for each potential above 0.8 V vs 0.8 V). Varying the applied potential also had a statistically significant effect on signal-to-noise ratios (S/N) and signal-to-background ratios (S/B) (right *y*-axis; [$F(7,24) = 18$, $P < 0.0001$] and [$F(7,24) = 270$; $P < 0.0001$], respectively). Increasing the applied potential to 1 V produced a significant reversal in signal-to-noise ($P < 0.01$ vs 0.8 V), while increasing E^{ox} to values > 0.9 V caused the previously maximal signal-to-background ratios to fall ($P < 0.01$ vs 0.8 V). Together, these findings suggest that application of an oxidative potential of 0.8 V at BDMs for chronoamperometry produces optimal integrated current by maximizing the serotonin-related current while minimizing contributions due to noise and background. Data represent serotonin concentration responses tested at four different BDMs. ** or $^{\dagger\dagger}P < 0.01$ vs corresponding value at 0.8 V. (B) Calibration curves are compared for BDMs and carbon fiber microelectrodes (CFMs) at serotonin concentrations ranging from 0.5 to 10 μM. Boron-doped diamond microelectrodes showed highly linear responses over the large concentration range tested ($r^2 = 0.9908$), in contrast to CFMs ($r^2 = 0.9579$), which showed a better correlation coefficient for a nonlinear fit to an exponential function ($r^2 = 0.9789$). Repeated measures two-way ANOVA revealed a significant interaction between serotonin concentration and electrode type [$F(4,50) = 76$, $P < 0.001$] indicating that BDMs and CFMs did not respond similarly to serotonin. Data were subsequently analyzed by two-tailed unpaired *t*-tests. CFMs showed significantly lower current responses per unit area at higher concentrations of serotonin (> 1.0 μM) compared to BDMs, possibly due to fouling of CFM surfaces (**$P < 0.01$ for 2.5 μM and 5.0 μM and ***$P < 0.001$ for 10 μM vs BDMs). Data represent oxidation current per unit area tested at six different BDMs and CFMs.

Table 1. Summary of Responses to Serotonin by Boron-Doped Diamond vs Bare or Nafion-Coated Carbon Fiber Microelectrodes[a]

	signal (nC/mm²)	S/N	S/B (%)	LOD (nM)
BDMs	8.4 ± 0.4	210 ± 30	17 ± 1	13 ± 3
Nafion-coated CFMs	6.8 ± 0.8	48 ± 7***	2.9 ± 0.4***	64 ± 8***
CMFs	5.3 ± 0.7*	48 ± 8***	2.7 ± 0.4***	67 ± 7***

[a] Boron-doped diamond microelectrodes (BDMs) showed significantly higher signal-to-noise and signal-to-background ratios and better limits of detection compared to those of Nafion-coated or bare carbon fiber microelectrodes. The absence of redox-active ionizable surface groups and lower concentrations of internal charge carriers in BDMs lead to lower background currents and noise. Data are mean responses to 1 μM serotonin ± SEMs ($n = 8 - 18$ samples per data point). The oxidative potential was 0.8 V for BDMs and 0.55 V for CFMs and Nafion-coated CFMs, while the reductive and resting potentials were 0 V for all electrodes. *$P < 0.05$ and ***$P < 0.001$ vs BDMs.

electrodes with anionic polymers, e.g., Nafion, or cleaning with organic solvents such as isopropanol (*57*, *58*, *62*, *63*). By contrast, BDMs exhibit minimal surface adsorption, primarily because of the absence of an extended π-electron system and a lack of polar carbon−oxygen surface groups.

Previously, Patel *et al.* investigated the ability of BDMs to resist fouling due to brief exposure (10 s) to high concentrations of serotonin (10 μM) comparing this to bare CFMs (*23*). Here, we extended those findings using conditions relevant to the present experiments, i.e., exposure to 10 μM serotonin or cell suspensions for 20 min, the time frame over which serotonin uptake occurs in the *ex vivo* experiments described below. Additionally, we compared the fouling properties of BDMs and CFMs to Nafion-coated CFMs. Boron-doped diamond microelectrodes showed significantly reduced fouling compared to both types of carbon fiber electrodes in the presence of high concentrations of serotonin or lymphocyte suspensions, as shown in Figures 4A and 4B, respectively. Exposure to 10 μM serotonin for 20 min resulted in significant decreases ($P < 0.001$) in electrode sensitivity for bare (−55 ± 5%) or Nafion-coated (−40 ± 7%) CFMs, whereas BDMs showed nonsignificant decreases in sensitivity that were less than 10% (Figure 4A). Cleaning BDMs with isopropanol led to a nearly complete recovery of sensitivity (97 ± 4%) indicating that serotonin reaction products are weakly adsorbed on these electrode surfaces (Figure 4A). By contrast, cleaning CFMs or Nafion-coated CFMs in isopropanol for 5 min did not significantly regenerate sensitivity ($P > 0.05$ vs after fouling).

Similarly, exposing electrodes to lymphocytes suspended in assay buffer (2 million cells/mL) for 20 min

DOI: 10.1021/cn900012y | ACS Chem. Neurosci. (2010), 1, 49–64

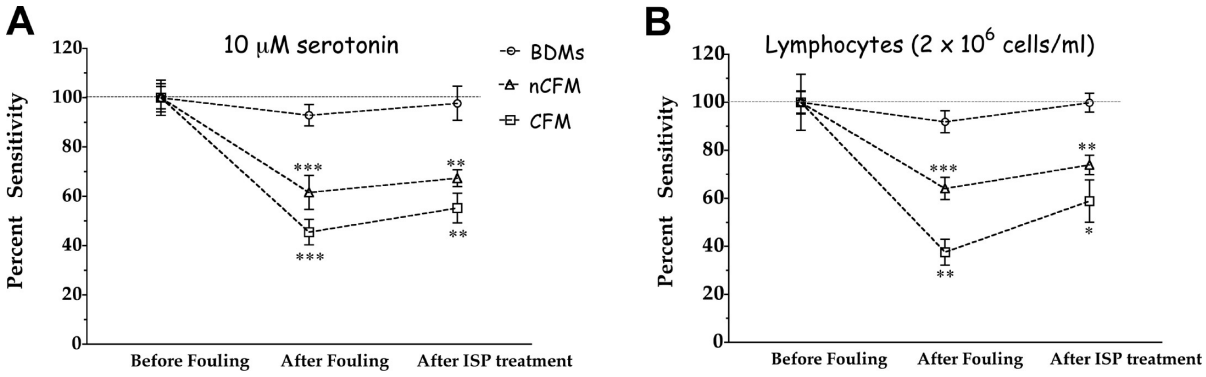

Figure 4. Electrode fouling at boron-doped diamond vs bare- and Nafion-coated carbon fiber microelectrodes. In (A), fouling was assessed in the presence of 10 μM serotonin, while in (B), fouling in response to exposure to lymphocytes was determined. Electrode responses were normalized to responses prior to exposure to fouling agents or cleaning with isopropanol (ISP). Data represent mean percent changes in electrode sensitivity ± SEMs ($N = 8$ samples per point after fouling; $N = 8-10$ samples per point after isopropanol). After calibration against 1 μM serotonin, electrodes were immersed in either 10 μM serotonin or lymphocytes in assay buffer for 20 min. Decreases in electrode sensitivity were determined by postcalibration. Fouled electrodes were then exposed to isopropanol for 5 min to determine the extent of electrode regeneration due to surface cleaning. Repeated measures two-way ANOVA revealed a significant interaction between treatment, i.e., fouling, cleaning, and electrode type (serotonin fouling [$F(4,42) = 11$, $P < 0.001$]; lymphocyte fouling [$F(4,46) = 5.4$, $P < 0.001$]) indicating that BDMs, CFMs, and Nafion-coated CFMs (N-CFMs) did not respond similarly to treatment. Data for each electrode type were subsequently analyzed by one-way ANOVA and Tukey's *post hoc* tests. Treatment had no effect on BDMs (serotonin fouling $F(2,14) = 1.2$, $P = 0.33$; lymphocyte fouling $F(2,14) = 2.1$, $P = 0.16$) indicating that these electrodes were resistant to fouling and that any small decreases in sensitivity were restored by isopropanol cleaning. By contrast, the effects of treatment were significant for CFMs (serotonin fouling $F(2,14) = 53$, $P < 0.001$; lymphocyte fouling $F(2,14) = 17$, $P < 0.001$) and Nafion-coated CFMs (serotonin fouling $F(2,14) = 19$, $P < 0.001$; lymphocyte fouling $F(2,14) = 15$, $P < 0.001$). For both of the latter, exposure to fouling agents significantly reduced electrode responsiveness. Moreover, isopropanol cleaning did not restore electrode sensitivity for CFMs and Nafion-coated CFMs ($P > 0.05$ vs after fouling). $^{**}P < 0.01$ and $^{***}P < 0.001$ vs before fouling.

resulted in significant decreases ($P < 0.001$) in sensitivity for bare CFMs (−60 ± 5%) and Nafion-coated CFMs (−35 ± 5%), compared to a nonsignificant 8.0 ± 5% decrease in sensitivity for BDMs (Figure 4B). Cleaning electrodes with isopropanol after biological fouling produced results similar to those obtained after exposure to serotonin, with only BDMs being completely regenerated (100 ± 2%). On the basis of these data and prior work in this developing field (*23*, *25*, *26*, *64*), it is evident that BDMs are significantly more resistant to fouling then CFMs, even when using common pre- and post-treatments for the latter. Thus, BDMs appear to be uniquely suited for measuring serotonin at higher concentrations and over longer time frames in biological preparations.

On the basis of our previous work in mouse brain synaptosomes (*4*, *6*), we anticipated that concentrations of serotonin >2 μM might be necessary to achieve maximal uptake rates in lymphocytes, hence our choice of higher concentrations of serotonin (10 μM) for the fouling study and upper limits of the calibration curves in the experiments described above. However, when we carried out initial uptake experiments in rhesus lymphocytes using BDMs and chronoamperometry, the data indicated that serotonin uptake in these cells is lower and that maximal uptake rates occurred at concentrations of serotonin <2 μM (see below). Although, CFMs show linear responses to serotonin at lower concentrations, the performance of BDMs was significantly better across the board with respect to responses to serotonin, reduced fouling, and reusability. Thus, we chose to use BDMs over CFMs or Nafion-coated CFMs for the experiments that follow.

Serotonin Is Actively Taken Up by Rhesus Lymphocytes

Transport of serotonin by SERT depends on sodium, chloride, and potassium concentration gradients maintained across the plasma membrane directly or indirectly by the Na^+/K^+-ATPase. Initially, substrate binding sites at SERT are accessible to the extracellular fluid allowing SERT to bind serotonin, Na^+, and Cl^- in a 1:1:1 stoichiometry (*65*). This leads to a conformation change, which results in the translocation of serotonin (and Na^+ and Cl^-) across the plasma membrane followed by its release into the cytoplasm. An intracellular potassium ion then binds to the SERT causing confirmation reversal. On the basis of this model of transport, a Na^+ gradient maintained across the plasma membrane ($[Na^+]_{out} \gg [Na+]_{in}$) is necessary to energetically drive the active transport of serotonin by SERT.

To investigate whether time-dependent decreases in amperometric current after the addition of serotonin to lymphocytes are due to an active transport process, we substituted equimolar LiCl for NaCl in the assay buffer and determined its effects on current with respect to time. Representative oxidative currents reflecting serotonin uptake by lymphocytes suspended in normal assay

DOI: 10.1021/cn900012y | *ACS Chem. Neurosci.* (2010), *1*, 49–64

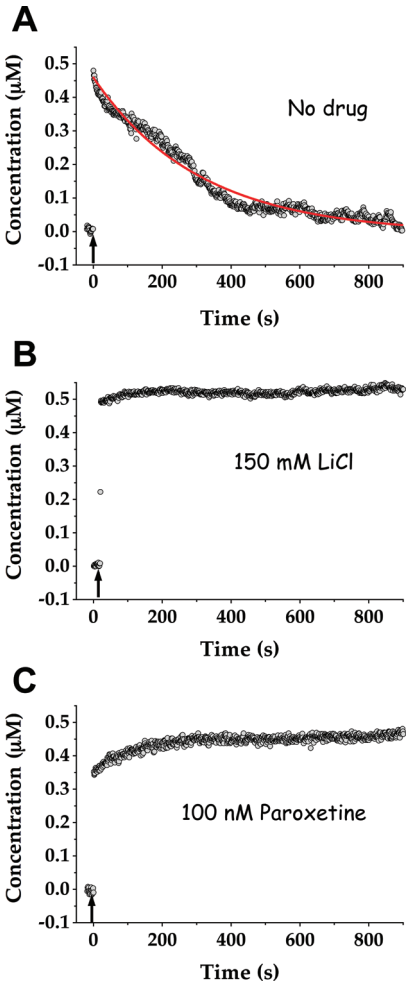

Figure 5. Active transport of serotonin in rhesus lymphocytes. In (A), lymphocytes were maintained in assay buffer containing 150 mM Na^+, while in (B), 150 mM Li^+ was substituted for Na^+. In (C), lymphocytes were preincubated for 45 min with the serotonin-selective reuptake inhibitor paroxetine (100 nM). Current was measured for 50 s prior to adding 0.5 μM serotonin ($t = 0$). On the basis of electrode calibration, integrated currents were converted to serotonin concentrations and then plotted with respect to time. For measurable uptake, curves were fit to a one-site exponential decay function (red line). The initial uptake rate in A was 3.9 pmol serotonin/million cells·min.

buffer containing 150 mM Na^+ vs assay buffer devoid of Na^+ are compared in Figure 5A and B, respectively. In the presence of sodium, suspensions of rhesus lymphocytes (2−4 million cells/mL) cleared 0.5 μM serotonin in ~15 min, as evidenced by a return of the oxidative current to baseline (Figure 5A). The mean uptake rate for pooled mixed-genotype lymphocytes was 3.3 ± 0.5 pmol serotonin/million cells-min ($N = 6$). By contrast, in the absence of extracellular sodium, the current remained constant with respect to time over the course of 15 min after the addition of 0.5 μM serotonin (Figure 5B). The latter was repeated using three independent lymphocyte samples and three different BDMs, and in each case, the experiment produced similar results. These results support the hypothesis that decreases in oxidative current after serotonin addition to lymphocytes are due to a Na^+-dependent active uptake mechanism.

Other Na^+- dependent plasma membrane transporters putatively expressed by lymphocytes, such as the dopamine transporter, have the capacity to transport serotonin, albeit with considerably lower affinity for serotonin than SERT (*66*, *67*). Paroxetine, a high affinity SSRI (K_i = 10 nM for SERT) (*68*), was used to investigate whether decreases in current after the addition of serotonin to lymphocytes are specifically due to SERT activity. Samples of rhesus peripheral blood lymphocytes were divided, and half of each sample was incubated with 100 nM paroxetine in assay buffer for 45 min, while the other half remained in assay buffer (*4*, *6*). Both samples were then resuspended in freshly oxygenated assay buffer. A representative serotonin uptake curve after paroxetine pretreatment is shown in Figure 5C. Oxidative current was monitored for 20 min after the addition of 0.5 μM serotonin to lymphocyte suspensions. No serotonin clearance was observed in lymphocytes preincubated with paroxetine compared to that in lymphocytes preincubated in assay buffer alone. These data suggest that SERT is primarily responsible for taking up serotonin in lymphocytes, resulting in time-dependent decreases in extracellular serotonin detected by chronoamperometry. Paroxetine preincubation experiments were performed on three separate days using separate frozen stocks of pooled lymphocytes and different BDMs with similar results each day.

Reduced Serotonin Uptake in Peripheral Blood Lymphocytes Is Associated with the Short Allele of the Rhesus *5-HTTLPR*

Rhesus macaques express a promoter polymorphism that is evolutionarily related to the human *5-HTTLPR*; however, studies have not been carried out to investigate serotonin uptake with respect to the rhesus gene variant. Here, we assessed SERT function in native (nontransformed) lymphocytes and observed allele-specific decreases in serotonin uptake associated with the short form of the *rh5-HTTLPR* (Figure 6). Serotonin uptake rates were significantly decreased by 30% in lymphocytes from monkeys with the *s*/*s* genotype ($P < 0.001$) and 25% in the *s*/*long l* genotype ($P < 0.05$) compared to those in animals with the *l*/*l* genotype. Thus, similar to the *h5-HTTLPR*, serotonin uptake is decreased in peripheral blood cells isolated from adult animals carrying the short *rh5-HTTLPR* allele, which is hypothesized to be associated with decreased SERT expression.

Serotonin uptake rates and SERT protein levels have each been evaluated in human transformed lymphoblasts and platelets with respect to the *h5-HTTLPR*. Lesch *et al.* first reported a decrease in serotonin

DOI: 10.1021/cn900012y | *ACS Chem. Neurosci.* (2010), *1*, 49–64

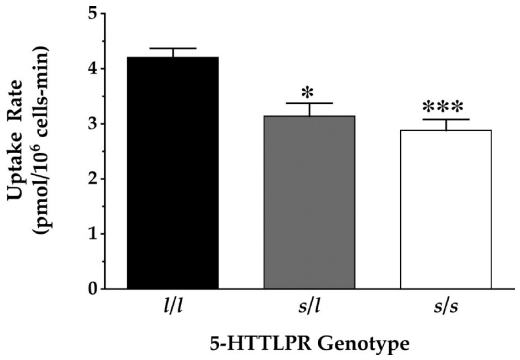

Figure 6. Differential uptake of serotonin by rhesus lymphocytes with respect to the *rh5-HTTLPR*. Uptake rates for 0.5 μM serotonin were significantly lower in lymphocytes obtained from monkeys with the *s*/*s* ($P < 0.01$) or *s*/*l* ($P < 0.05$) genotypes compared to those with *l*/*l* genotype. Data are mean initial uptake rates ± SEMs ($N = 6$ for *s*/*s* and *l*/*l*; $N = 3$ for *s*/*l*). *$P < 0.05$ and **$P < 0.001$ vs *l*/*l* genotype.

uptake and SERT binding associated with the *s* allele in human transformed lymphoblastoid cell lines (*31*). Later studies on serotonin transport in human platelets corroborated these findings (*69*−*71*), with the exception of one study by Kaiser *et al.* (*72*). However, most studies on SERT binding as a measure of SERT protein levels in platelets have failed to find decreases associated with the *h5-HTTLPR s* allele (*69*, *70*, *73*) and only Stoltenberg *et al.* reported a reduction in SERT binding in *s* allele platelets (*74*). It is not clear what the underlying reasons are for the discrepancies between SERT binding and function nor what biological significance this may have.

Uptake studies in human platelets and lymphoblastoid cells have utilized radiochemical assay to assess serotonin uptake rates. However, we have shown that kinetic parameters obtained using this technique underestimate maximal uptake rates in brain synaptosomes because of a loss of transported serotonin occurring during high pressure vacuum filtration (*6*). Here, we observe uptake rates in rhesus primary lymphocytes by chronoamperometry comparable to [^{3}H]-serotonin uptake rates reported in platelets. Future studies will be needed to determine whether intact cells retain transported serotonin during vacuum filtration unlike synaptosomes, which are derived from previously disrupted neurons. Gaining a better understanding of these technical aspects will allow more accurate comparisons of uptake rates in intact cells obtained by radiochemical assay vs voltammetry methods.

Similar to studies in peripheral cells, studies on the effects of the *5-HTTLPR* in human brain have resulted in conflicting findings. Little *et al.* reported a significant decrease in SERT binding in postmortem midbrain associated with the *s*/*l* but not the *s*/*s* genotype compared to the *l*/*l* genotype; however, the number of *s*/*s* individuals investigated was small (*44*). By contrast, Naylor and co-workers observed no significant differences with respect to the *h5-HTTLPR* genotype in postmortem hippocampus (*75*). Studies measuring *in vivo* SERT binding potential by PET or single photon emission computed tomography (SPECT) have likewise yielded mixed results. Heinz *et al.* observed an *s* allele-dependent decrease in SERT binding in human midbrain (*76*). However, van Dyke *et al.* found *increased* binding in *s*/*s* individuals compared to that in *s*/*l* individuals in the brain stem (*77*). Others have reported no differences in SERT binding with respect to *h5-HTTLPR* genotype using PET or SPECT (*46*, *78*, *79*). In rhesus monkeys, SERT binding evaluated by SPECT was not significantly different with respect to *rh5-HTTLPR* genotype in the brain stem (*80*). The low resolution of PET or SPECT imaging might account for these mostly negative findings *in vivo*.

Mice and rats with reduced SERT expression have also been produced to investigate the effects of SERT deficiency on neurochemistry, neurophysiology, neuropharmacology, and behavior (*4*−*6*, *28*−*30*, *39*, *54*, *81*−*84*). Rodents with constitutive loss of SERT expression exhibit increases in anxiety-related behavior (*28*, *82*, *83*) that bears resemblance to increases in anxiety-related personality traits reported in humans carrying one or two copies of the *h5-HTTLPR s* allele. Moreover, postnatal disruption of SERT function by administration of serotonin reuptake inhibiting antidepressants in mice and rats leads to an increased anxiety-related phenotype during adulthood (*85*−*87*). Together, these data from genetic and pharmacologic rodent models, when viewed particularly in light of the negative data on the *h5-HTTLPR* and its association with differential SERT binding in adult human brain and platelets, have led to the hypothesis that the effects of the *h5-HTTLPR* on SERT expression and function might be limited to key postnatal periods (*46*, *88*). Reduced serotonin uptake in early development is thought to alter the formation of neuronal circuits responsible for modulating anxiety-related behavior during adulthood.

In contrast to this hypothesis wherein the effects of the *5-HTTLPR* are limited to development, we observe significant differences in serotonin uptake rates associated with the *rh5-HTTLPR* in native rhesus lymphocytes obtained from adult animals using highly sensitive electrochemical methods. Our results strongly suggest that the *rh5-HTTLPR* influences SERT function not only during critical developmental periods but that these effects persist into adulthood. Previously, we and others have elucidated modest but biologically important differences in serotonin uptake rates in the brains of mice with partial constitutive reductions in SERT expression using chronoamperometry that are on the order of the differences in uptake rates observed here in rhesus lymphocytes. We hypothesize that the negative findings on the *h5-HTTLPR* and its association with SERT

DOI: 10.1021/cn900012y | *ACS Chem. Neurosci.* (2010), *1*, 49–64

expression and/or function described above might largely be due to the use of methods with low resolution for determining uptake rates, e.g., radiochemical uptake methods or *in vivo* SERT binding, e.g., PET or SPECT imaging. Understanding whether the effects of the *rh5-HTTLPR* and more importantly, the *h5-HTTLPR*, persist into adulthood will be critical for advancing our fundamental understanding of the mechanisms by which this ubiquitous gene variant influences the architecture of human personality. Moreover, these mechanisms are also important for interpreting large individual variations in treatment response to SSRIs (*41*) and for using SERT activity in peripheral lymphocytes as a biomarker for personalizing first-line treatments for patients suffering from depression and anxiety disorders.

Conclusions and Future Prospects

With recent advances in fabrication methods for thin-film boron-doped diamond (*22*) and reductions in the sizes of BDMs (*64*, *89*), these electrodes are becoming increasingly suited for making measurements of neurotransmitters in biological environments with the high temporal and spatial resolution needed to elucidate smaller magnitude changes that are nonetheless of principal biological significance. The unique surface chemistry of BDMs imparts excellent resistance to fouling. However, unlike coatings such as Nafion, they do not afford intrinsic advantages for detecting cationic monoamine neurotransmitters over anionic metabolites (*90*), the latter of which are typically encountered at high concentrations *in vivo*. However, a number of BDM surface modifications have been reported to provide selectivity along these lines. Anodized BDMs show separation of peak oxidative potentials for dopamine vs ascorbate, facilitating selective dopamine detection (*89*, *91*). Weng *et al.* electrodeposited gold clusters on boron-doped diamond electrodes followed by self-assembled monolayers of mercaptoacetic acid, and together, these modifications both enhanced the separation of oxidative peak potentials between dopamine and ascorbate and increased the limits of detection for dopamine (*92*). Moreover, permselective films on boron-doped diamond have been used to selectively detect dopamine or serotonin in the presence of ascorbate (*93*, *94*). In the present study, selectivity for cations was not an issue since we controlled the composition of the extracellular solution containing serotonin.

We conclude that reduced SERT function is associated with the short allele of the *rh5-HTTLPR* in peripheral blood lymphocytes isolated from adult rhesus monkeys. Our results illustrate further the sensitivity of chronoamperometry for differentiating serotonin uptake rates. They also demonstrate the effectiveness of boron-doped diamond microelectrodes for measuring serotonin uptake in peripheral cells natively expressing SERT. However, a number of key questions will need to be answered prior to determining whether peripheral lymphocytes can be used as potential biomarkers to reveal alterations in central SERT function associated with genetic variability and/or antidepressant responses in humans. First, are *rh5-HTTLPR*-related differences in SERT function associated with corresponding changes in SERT mRNA and/or protein levels in rhesus lymphocytes? Second, are *rh5-HTTLPR*-associated effects in the periphery paralleled in the brain, or are the ramifications of the *5-HTTLPR* for anxiety-related personality traits and susceptibility to stress-related psychiatric disorders based on developmental central effects possibly interacting with adult peripheral alterations in serotonin transport? Third, how does the situation in rhesus monkeys compare to that in humans? The *rh5-HTTLPR*, in combination with electrochemical methods, provides many unique advantages for investigating some of these questions, including the possibility of carrying out *in vivo* neurochemical studies to determine associations between peripheral and central SERT function in monkeys (*64*, *89*).

To understand at the molecular level factors that influence susceptibility to anxiety disorders and depression, as well as drug mechanisms and efficacy, elucidating the effects of SERT polymorphisms, alone and in combination, on SERT expression and function will be necessary. Boron-doped diamond electrodes when used in combination with voltammetry can be used to detect modest change in serotonin uptake rates. Furthermore, the application of these methods to peripherally accessible tissues such as lymphocytes together comprise a powerful system to explore and to understand interneuronal chemical communication.

Experimental Procedures

Lymphocyte Preparations

Venous blood was collected from Chinese rhesus macaques (*Macaca mulatta*) under anesthesia. Experimental protocols strictly adhered to National Institutes of Health guidelines and were approved by the University of Pittsburgh School of Medicine Institutional Animal Care and Use Committee. High molecular weight genomic DNA was isolated by standard methods, and genotyping of the *rh5-HTTLPR* was carried out as described by Lesch *et al.* (*47*). Monkeys for the present study were selected from a cohort of 42 animals based on their *rh5-HTTLPR* genotype. Study animals were 6.9 ± 0.1 years of age and weighed 7.8 ± 0.4 kg at the time of blood collection. Genotypes were $N = 6$ for *l*/*l*, $N = 3$ for *s*/*l*, and $N = 6$ for *s*/*s*. Blood was collected from additional monkeys that had not been genotyped, and these blood samples were mixed together. Lymphocytes isolated from this pooled blood were used for protocol development and other experiments that were not dependent on genotype.

DOI: 10.1021/cn900012y | *ACS Chem. Neurosci.* (2010), *1*, 49–64

Peripheral blood lymphocytes were isolated from anticoagulated blood by Ficoll−Paque PLUS gradient centrifugation according to the manufacturer's instructions (GE Healthcare, Piscataway, NJ). Whole blood was diluted with RPMI media (Invitrogen Corporation, Carlsbad, CA) and added into Accuspin tubes (Sigma Aldrich, St. Louis, MO) containing Ficoll (GE Healthcare, Piscataway, NJ) and then centrifuged for 25−30 min at 900 g at room temperature. The entire top white layer was collected in 5% RPMI media followed by centrifugation at 900*g* for 10 min. The supernatant was then resuspended in 10−20 mL of 10% RPMI. If detected, red blood cells were lysed, and the samples were vortexed and rinsed with fresh 10% RPMI and centrifuged for an additional 10 min at 900*g*. Cell pellets were brought up in a freezing media (RPMI containing heat inactivated fetal bovine serum and 10% dimethylsulfoxide) and were placed at −20 °C for 1 h prior to freezing overnight in a Mr. Frosty (Thermo Fisher Scientific, Rochester, NY) at −80 °C. Long-term storage was in liquid nitrogen.

Representative frozen samples were thawed in assay buffer, and cell type and cell survival were analyzed by flow cytometry. Forward and side scatter plots indicated that cell populations were predominantly lymphocytes containing a few monocytes with no evidence of platelets or red blood cells. Trypan blue exclusion was also used to assess cell survival (see below).

Electrode Fabrication

Boron-doped diamond microelectrodes were fabricated using previously described procedures (*22*). Briefly, boron-doped diamond was deposited over chemically etched platinum wires using microwave-assisted chemical vapor deposition (1.5 kW, 2.54 GHz, ASTeX, Woburn, MA) to produce cylindrical electrode geometries. Boron doping was achieved during the vapor deposition process by adding 10 ppm B_2H_6 to 0.5% CH_4/H_2. After deposition, each diamond-coated platinum wire was glued to a copper wire using silver epoxy, and the joint was sealed in a polypropylene pipet tip using a heat gun.

Carbon fiber microelectrodes (CFMs) were prepared as described previously with minor modifications (*4*, *6*). Some electrodes were coated with Nafion, a perfluorinated ion-exchange polymer used to reduce fouling (*57*). Electrodes were cleaned with isopropanol, and Nafion was applied by dipping CFMs for 30 s followed by drying at 100 °C for 5 min between coats. The coating process was repeated 6 times, and coating effectiveness was evaluated by challenging electrodes with 100 μM ascorbate. Only Nafion-coated electrodes with selectivity for serotonin over ascorbate > 1000:1 were used in subsequent experiments.

Reference electrodes were fabricated by electrochemically coating silver wires (Alfa Aesar, Ward Hill, MA) with AgCl. Silver wires were immersed in 3 M HCl saturated with NaCl, and a 9 V potential was applied for 5 min.

Electrochemistry

Cyclic voltammetry and high-speed chronoamperometry were performed using a Universal Electrochemistry Instrument and TarHeel CV software, version 1.0 (University of North Carolina, Chapel Hill, NC). Chronoamperometry raw data from the TarHeel CV software were further analyzed using a custom software module, ChronoAmp, written in-house. For chronoamperometry, a 1 Hz square wave step potential was applied to the working electrode, which consisted of an oxidative potential at 0.8 V for BDD electrodes or 0.55 V for CFMs, except where otherwise indicated. The oxidative potential was applied for 100 ms followed by a 0 V reductive potential for 100 ms (Figure 7B). The potential was held at 0 V for an additional 800 ms to reduce fouling due to serotonin and its oxidation products (delayed-pulse mode) (*95*). Potentials were applied with respect to Ag/AgCl reference electrodes. The last 80 ms of the oxidative and reductive phases representing faradaic current were integrated.

Integrated current values prior to the addition of serotonin were defined as background current, while integrated current after the addition of serotonin was defined as total current. The oxidation and reduction currents due to serotonin (i.e., signal) were calculated by subtracting background currents from total currents. Background-subtracted currents were plotted with respect to time (Figure 7C). Noise was calculated as the standard deviation of the background current measured over 10 scans. Limits of detection were defined as the concentrations of serotonin needed to generate signals equivalent to three times the noise values. In addition to background and total current, the current for 80 ms just prior to the application of the oxidative pulse was integrated to calculate the drift in background current and voltage (IR) drop due to resistance in the circuit. The drift current was subtracted from the oxidative and reductive currents to minimize the contribution of electrode drift and voltage drop to the determination of faradic current resulting from serotonin.

For evaluation of responses to 10 μM serotonin by cyclic voltammetry, BDMs or CFMs were held at −0.4 V with respect to Ag/AgCl reference electrodes and scanned from −0.4 to 1.0 V to −0.4 at 1 V/s every 10 s. Background and oxidative currents were determined at the potential needed to produce half maximal current in the presence of serotonin ($E_{1/2}^{ox}$) at the respective electrodes. All cyclic voltammograms used to measure signal and background currents were averaged over 10 scans.

Experiments were performed in 12-well polystyrene plates (BD Biosciences, San Jose, CA). Reference and working electrodes were carefully lowered into each well containing assay buffer (150 mM NaCl, 5 mM KCl, 1.2 mM $MgCl_2$, 5 mM glucose, 10 mM HEPES, and 2 mM $CaCl_2$, pH 7.4) or lymphocytes suspended in assay buffer, and the background current was monitored (Figure 7A). Data collection began when the background current stabilized, i.e., changes in current were < 0.1 nA for BDMs or < 0.2 nA for CFMs for a minimum of 100 s. The background current was then recorded for 50 s followed by injection of serotonin into the assay buffer. Solutions of lymphocytes or buffer were briefly stirred, and the current was recorded for an additional 120 s for calibration experiments or 1200 s for uptake experiments without further stirring. Electrodes were calibrated prior to each experiment against known concentrations of serotonin in assay buffer (0.1−1 μM unless otherwise noted), and the linearity of the responses were calculated. Electrodes were also calibrated after each experiment to determine changes in electrode sensitivity due to fouling.

Serotonin Uptake

Frozen lymphocytes (~10 million cells/mL) were thawed by adding 12−15 mL of 37 °C assay buffer. Small volumes

DOI: 10.1021/cn900012y | *ACS Chem. Neurosci.* (2010), *1*, 49–64

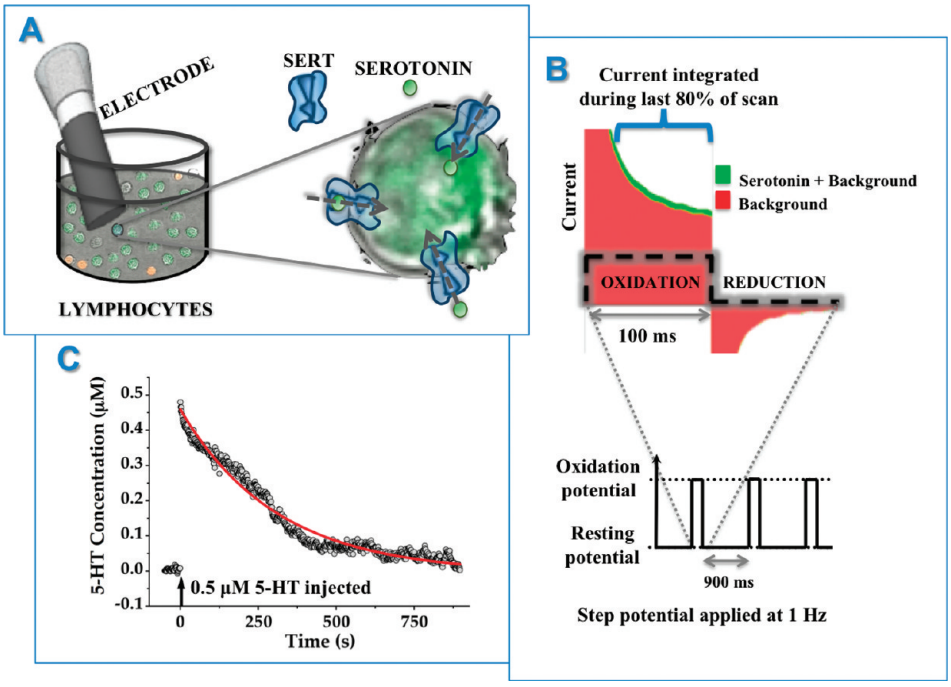

Figure 7. Chronoamperometry in lymphocytes. (A) Electrodes were immersed in solutions of lymphocytes that natively express the serotonin transporter (SERT). Decreases in extracellular serotonin concentrations due to uptake into lymphocytes by SERT were monitored electrochemically. (B) For chronoamperometry, a 1 Hz square wave step potential was applied to the working electrode for 100 ms. The current produced during the last 80 ms of the oxidation pulse representing faradaic current was integrated and background subtracted, and used to estimate the serotonin concentration present in the extracellular solution on a second-by-second basis. (C) Extracellular serotonin concentrations were plotted against time. Uptake of serotonin by SERT resulted in a decrease in extracellular serotonin over time. Fitting these data using an exponential decay function (red line) provides initial serotonin uptake rates.

(200 μL) of lymphocytes were used for counting live cells using Trypan blue exclusion. On average, 75% of the cells were alive after the thawing procedure. Lymphocytes were then centrifuged at 340*g* for 7 min. Pellets containing lymphocytes were resuspended by gently vortexing in assay buffer to produce final concentrations of 2−4 million cells/mL except where otherwise noted. Prior to each experiment, numbers of live cells were determined, and uptake rates were normalized per million live cells. Solutions of lymphocytes were kept at 4 °C for no more than 4 h before uptake experiments.

Immediately prior to measuring serotonin uptake, lymphocytes were centrifuged at 340*g* for 7 min. Freshly oxygenated assay buffer saturated with 95% O_2/5% CO_2 by bubbling the gas mixture for at least 30 min was utilized at room temperature for all experiments. Cells were resuspended in an appropriate amount of assay buffer by gently vortexing. In some experiments, frozen lymphocytes were thawed in oxygenated assay buffer containing 150 mM LiCl substituted for NaCl. Prior to measuring uptake, half of these lymphocytes were resuspended in LiCl-substituted oxygenated assay buffer and the other half in normal oxygenated assay buffer to investigate Na^+-dependent uptake. In other experiments, divided solutions of lymphocytes were preincubated for 45 min with paroxetine (100 nM) in assay buffer or assay buffer alone to investigate the effects of SERT inhibition on uptake.

Chemicals

Serotonin, paroxetine, Nafion, and chemicals for lymphocyte isolation were purchased from Sigma-Aldrich (St. Louis, MO). All chemicals used for assay buffer preparation were purchased from VWR (West Chester, PA).

Data Analysis and Statistics

For chronoamperometry experiments, the first order rate constant, b (s^{-1}), was determined by fitting serotonin clearance data to the following exponential decay function (*96*):

$$y = f(t) = A \times e^{-b(t-t_0)} \quad (1)$$

where y is the serotonin concentration (μM) at any given time (t), t_o is the time (s) at the start of uptake, and A is the concentration of serotonin (μM) at t_0.

Initial serotonin uptake rates, v (μM/s), were then calculated using the following formula:

$$v = b \times A \quad (2)$$

Uptake rates were determined to be not detectable (negligible serotonin uptake) in cases where a $< 10\%$ decrease in current occurred over 20 min after serotonin injection.

Data comparing two means were analyzed using two-tailed unpaired *t*-tests. One-way analysis of variance (ANOVA) was used in cases where more than two means were compared, followed by either Dunnett's Multiple Comparison or Tukey's *post hoc* tests. Two-way ANOVA with repeated measures was used to analyze calibration data using serotonin concentrations as the repeated measure and to analyze fouling data with treatment as the repeated measure. Calibration data were also analyzed by multiple regression analysis and nonlinear curve

DOI: 10.1021/cn900012y | *ACS Chem. Neurosci.* (2010), *1*, 49–64

fitting. All statistical analyses were performed using GraphPad Prism v.4 for Mac (GraphPad Software, La Jolla, CA). All values are expressed as means ± standard errors of the mean (SEMs), with differences of $P < 0.05$ considered statistically significant. Significant differences are denoted in the figures as $^{*}P < 0.05$, $^{**}P < 0.01$, $^{***}P < 0.001$, and $^{\dagger\dagger}P < 0.01$.

Author Information

Corresponding Author

*To whom correspondence should be addressed. Anne Milasincic Andrews, Semel Institute for Neuroscience & Human Behavior, University of California, Los Angeles, 760 Westwood Plaza 68/226A, Los Angeles, CA 90024-1759. E-mail: ama@cnsi.ucla.edu.

Notes

The content is solely the responsibility of the authors and does not necessarily represent the official views of the National Institute of Mental Health or the National Institutes of Health.

Acknowledgment

We would like to remember Professor Peter C. Eklund, who contributed greatly to our understanding of carbon in its many forms. We are grateful to Dr. Charles Bradberry for guidance regarding nonhuman primates and Drs. Andrew Ewing and Michael Heien for advice on electrochemical methods. We also acknowledge Ms. Stefanie Altieri and Mr. Brendan Beikmann for assistance with the experiments. This project was supported by funding from the National Institute of Mental Health (MH064756 to AMA).

References

1. Michael, A. C., and Borland, L. M., Eds. (2007) *Electrochemical Methods of Neurotransmitter Analysis*, CRC Press LLC, Boca Raton, FL.

2. Parikh, V., Kozak, R., Martinez, V., and Sarter, M. (2007) Prefrontal acetylcholine release controls cue detection on multiple timescales. *Neuron 56*, 141–154.

3. Walker, E., Wang, J., Hamdi, N., Monbouquette, H. G., and Maidment, N. T. (2007) Selective detection of extracellular glutamate in brain tissue using microelectrode arrays coated with over-oxidized polypyrrole. *Analyst 132*, 1107–1111.

4. Perez, X. A., and Andrews, A. M. (2005) Chronoamperometry to determine differential reductions in uptake in brain synaptosomes from serotonin transporter knockout mice. *Anal. Chem. 77*, 818–826.

5. Montañez, S., Owens, W. A., Gould, G. G., Murphy, D. L., and Daws, L. C. (2003) Exaggerated effect of fluvoxamine in heterozygote serotonin transporter knockout mice. *J. Neurochem. 86*, 210–219.

6. Perez, X. A., Bianco, L. E., and Andrews, A. M. (2006) Filtration disrupts synaptosomes during radiochemical analysis of serotonin uptake: Comparison with chronoamperometry in SERT knockout mice. *J. Neurosci. Methods 154*, 245–255.

7. Bengel, D., Murphy, D. L., Andrews, A. M., Wichems, C. H., Feltner, D., Heils, A., Mossner, R., Westphal, H., and Lesch, K. P. (1998) Altered brain serotonin homeostasis and locomotor insensitivity to 3,4-methylenedioxymethamphetamine ("Ecstasy") in serotonin transporter-deficient mice. *Mol. Pharmacol. 53*, 649–655.

8. Kita, J. M., and Wightman, R. M. (2008) Microelectrodes for studying neurobiology. *Curr. Opin. Chem. Biol. 12*, 1–6.

9. Wightman, R. M. (2006) Detection technologies. Probing cellular chemistry in biological systems with microelectrodes. *Science 311*, 1570–1574.

10. Bath, B. D., Martin, H. B., Wightman, R. M., and Anderson, M. R. (2001) Dopamine adsorption at surface modified carbon-fiber electrodes. *Langmuir 17*, 7032–7039.

11. Yang, H. H., and McCreery, R. L. (1999) Effects of surface monolayers on the electron-transfer kinetics and adsorption of methyl viologen and phenothiazine derivatives on glassy carbon electrodes. *Anal. Chem. 71*, 4081–4087.

12. Chen, P. H., and McCreery, R. L. (1996) Control of electron transfer kinetics at glassy carbon electrodes by specific surface modification. *Anal. Chem. 68*, 3958–3965.

13. Chen, P. H., Fryling, M. A., and Mccreery, R. L. (1995) Electron-transfer kinetics at modified carbon electrode surfaces - the role of specific surface sites. *Anal. Chem. 67*, 3115–3122.

14. Dryhurst, G. (1990) Applications of electrochemistry in studies of the oxidation chemistry of central nervous system indoles. *Chem. Rev. 90*, 795–811.

15. Wrona, M. Z., and Dryhurst, G. (1988) Further insights into the oxidation chemistry of 5-hydroxytryptamine. *J. Pharm. Sci. 77*, 911–917.

16. Wrona, M. Z., and Dryhurst, G. (1990) Electrochemical oxidation of 5-hydroxytryptamine in aqueous solution at physiological pH. *Bioorg. Chem. 18*, 291–317.

17. Anastassiou, C. A., Patel, B. A., Arundell, M., Yeoman, M. S., Parker, K. H., and O'Hare, D. (2006) Subsecond voltammetric separation between dopamine and serotonin in the presence of ascorbate. *Anal. Chem. 78*, 6990–6998.

18. Bennett, J. A., Wang, J. A., Show, Y., and Swain, G. M. (2004) Effect of sp(2)-bonded nondiamond carbon impurity on the response of boron-doped polycrystalline diamond thin-film electrodes. *J. Electrochem. Soc. 151*, E306–E313.

19. Fischer, A. E., Show, Y., and Swain, G. M. (2004) Electrochemical performance of diamond thin-film electrodes from different commercial sources. *Anal. Chem. 76*, 2553–2560.

20. Sarada, B. V., Rao, T. N., Tryk, D. A., and Fujishima, A. (2000) Electrochemical oxidation of histamine and serotonin at highly boron-doped diamond electrodes. *Anal. Chem. 72*, 1632–1638.

21. Xu, J. S., Granger, M. C., Chen, Q. Y., Strojek, J. W., Lister, T. E., and Swain, G. M. (1997) Boron-doped diamond thin-film electrodes. *Anal. Chem. 69*, A591–A597.

22. Park, J., Quaiserova-Mocko, V., Patel, B. A., Novotny, M., Liu, A., Bian, X., Galligan, J. J., and Swain, G. M. (2008)

DOI: 10.1021/cn900012y | *ACS Chem. Neurosci.* (2010), *1*, 49–64

Diamond microelectrodes for *in vitro* electroanalytical measurements: current status and remaining challenges. *Analyst 133*, 17–24.

23. Patel, B. A., Bian, X., Quaiserova-Mocko, V., Galligan, J. J., and Swain, G. M. (2007) *In vitro* continuous amperometric monitoring of 5-hydroxytryptamine release from enterochromaffin cells of the guinea pig ileum. *Analyst 132*, 41–47.

24. Chau, R. M., and Patel, B. A. (2009) Determination of serotonin, melatonin and metabolites in gastrointestinal tissue using high-performance liquid chromatography with electrochemical detection. *Biomed. Chromatogr. 23*, 175–181.

25. Patel, B. A. (2008) Continuous amperometric detection of co-released serotonin and melatonin from the mucosa in the ileum. *Analyst 133*, 516–524.

26. Bian, X., Patel, B., Dai, X., Galligan, J. J., and Swain, G. (2007) High mucosal serotonin availability in neonatal guinea pig ileum is associated with low serotonin transporter expression. *Gastroenterology 132*, 2438–2447.

27. Blakely, R. D., Defelice, L. J., and Galli, A. (2005) Biogenic amine neurotransmitter transporters: Just when you thought you knew them. *Physiology 20*, 225–231.

28. Murphy, D. L., Fox, M. A., Timpano, K. R., Moya, P. R., Ren-Patterson, R., Andrews, A. M., Holmes, A., Lesch, K. P., and Wendland, J. R. (2008) How the serotonin story is being rewritten by new gene-based discoveries principally related to *SLC6A4*, the serotonin transporter gene, which functions to influence all cellular serotonin systems. *Neuropharmacology 55*, 932–960.

29. Trigo, J. M., Renoir, T., Lanfumey, L., Hamon, M., Lesch, K. P., Robledo, P., and Maldonado, R. (2007) 3,4-methylenedioxymethamphetamine self-administration is abolished in serotonin transporter knockout mice. *Biol. Psychiatry 62*, 669–679.

30. Sora, I., Hall, F. S., Andrews, A. M., Itokawa, M., Li, X. F., Wei, H. B., Wichems, C., Lesch, K. P., Murphy, D. L., and Uhl, G. R. (2001) Molecular mechanisms of cocaine reward: Combined dopamine and serotonin transporter knockouts eliminate cocaine place preference. *Proc. Natl. Acad. Sci. U.S.A. 98*, 5300–5305.

31. Lesch, K. P., Bengel, D., Heils, A., Sabol, S. Z., Greenberg, B. D., Petri, S., Benjamin, J., Muller, C. R., Hamer, D. H., and Murphy, D. L. (1996) Association of anxiety-related traits with a polymorphism in the serotonin transporter gene regulatory region. *Science 274*, 1527–1531.

32. Wendland, J. R., Martin, B. J., Kruse, M. R., Lesch, K. P., and Murphy, D. L. (2006) Simultaneous genotyping of four functional loci of human *SLC6A4*, with a reappraisal of *5-HTTLPR* and rs25531. *Mol. Psychiatry 11*, 224–226.

33. Wendland, J. R., Moya, P. R., Kruse, M. R., Ren-Patterson, R. F., Jensen, C. L., Timpano, K. R., and Murphy, D. L. (2008) A novel, putative gain-of-function haplotype at *SLC6A4* associates with obsessive-compulsive disorder. *Hum. Mol. Genet. 17*, 717–723.

34. Hu, X. Z., Lipsky, R. H., Zhu, G., Akhtar, L. A., Taubman, J., Greenberg, B. D., Xu, K., Arnold, P. D., Richter, M. A., Kennedy, J. L., Murphy, D. L., and Goldman, D. (2006) Serotonin transporter promoter gain-of-function genotypes are linked to obsessive-compulsive disorder. *Am. J. Hum. Genet. 78*, 815–826.

35. Sutcliffe, J. S., Delahanty, R. J., Prasad, H. C., McCauley, J. L., Han, Q., Jiang, L., Li, C., Folstein, S. E., and Blakely, R. D. (2005) Allelic heterogeneity at the serotonin transporter locus (*SLC6A4*) confers susceptibility to autism and rigid-compulsive behaviors. *Am. J. Hum. Genet. 77*, 265–279.

36. Prasad, H. C., Zhu, C. B., McCauley, J. L., Samuvel, D. J., Ramamoorthy, S., Shelton, R. C., Hewlett, W. A., Sutcliffe, J. S., and Blakely, R. D. (2005) Human serotonin transporter variants display altered sensitivity to protein kinase G and p38 mitogen-activated protein kinase. *Proc. Natl. Acad. Sci. U.S.A. 102*, 11545–11550.

37. Ozaki, N., Goldman, D., Kaye, W. H., Plotnicov, K., Greenberg, B. D., Lappalainen, J., Rudnick, G., and Murphy, D. L. (2003) Serotonin transporter missense mutation associated with a complex neuropsychiatric phenotype. *Mol. Psychiatry 8*, 933–936.

38. Zhang, Y. W., Gesmonde, J., Ramamoorthy, S., and Rudnick, G. (2007) Serotonin transporter phosphorylation by cGMP-dependent protein kinase is altered by a mutation associated with obsessive compulsive disorder. *J. Neurosci. 27*, 10878–10886.

39. Fox, M. A., Jensen, C. L., Gallagher, P. S., and Murphy, D. L. (2007) Receptor mediation of exaggerated responses to serotonin-enhancing drugs in serotonin transporter (SERT)-deficient mice. *Neuropharmacology 53*, 643–656.

40. Uher, R., and McGuffin, P. (2008) The moderation by the serotonin transporter gene of environmental adversity in the aetiology of mental illness: Review and methodological analysis. *Mol. Psychiatry 13*, 131–146.

41. Murphy, D. L., Lerner, A., Rudnick, G., and Lesch, K. P. (2004) Serotonin transporter: Gene, genetic disorders, and pharmacogenetics. *Mol. Interv. 4*, 109–123.

42. Little, K. Y., Zhang, L., and Cook, E. (2006) Fluoxetine-induced alterations in human platelet serotonin transporter expression: Serotonin transporter polymorphism effects. *J. Psychiatry Neurosci. 31*, 333–339.

43. Heils, A., Teufel, A., Petri, S., Stober, G., Riederer, P., Bengel, D., and Lesch, K. P. (1996) Allelic variation of human serotonin transporter gene expression. *J. Neurochem. 66*, 2621–2624.

44. Little, K. Y., McLaughlin, D. P., Zhang, L., Livermore, C. S., Dalack, G. W., McFinton, P. R., DelProposto, Z. S., Hill, E., Cassin, B. J., Watson, S. J., and Cook, E. H. (1998) Cocaine, ethanol, and genotype effects on human midbrain serotonin transporter binding sites and mRNA levels. *Am. J. Psychiatry 155*, 207–213.

45. Lim, J. E., Papp, A., Pinsonneault, J., Sadee, W., and Saffen, D. (2006) Allelic expression of serotonin transporter (SERT) mRNA in human pons: Lack of correlation with the polymorphism SERTLPR. *Mol. Psychiatry 11*, 649–662.

46. Parsey, R. V., Hastings, R. S., Oquendo, M. A., Hu, X., Goldman, D., Huang, Y. Y., Simpson, N., Arcement, J., Huang, Y., Ogden, R. T., Van Heertum, R. L., Arango, V., and Mann, J. J. (2006) Effect of a triallelic functional polymorphism of the serotonin-transporter-linked promoter

DOI: 10.1021/cn900012y | *ACS Chem. Neurosci.* (2010), *1*, 49–64

region on expression of serotonin transporter in the human brain. *Am. J. Psychiatry 163*, 48–51.

47. Lesch, K. P., Meyer, J., Glatz, K., Flugge, G., Hinney, A., Hebebrand, J., Klauck, S. M., Poustka, A., Poustka, F., Bengel, D., Mossner, R., Riederer, P., and Heils, A. (1997) The 5-HT transporter gene-linked polymorphic region (*5-HTTLPR*) in evolutionary perspective: Alternative biallelic variation in rhesus monkeys. *J. Neural Transm. 104*, 1259–1266.

48. Wendland, J. R., Lesch, K. P., Newman, T. K., Timme, A., Gachot-Neveu, H., Thierry, B., and Suomi, S. J. (2006) Differential functional variability of serotonin transporter and monoamine oxidase A genes in macaque species displaying contrasting levels of aggression-related behavior. *Behav. Genet. 36*, 163–172.

49. Barr, C. S., Newman, T. K., Becker, M. L., Champoux, M., Lesch, K. P., Suomi, S. J., Goldman, D., and Higley, J. D. (2003) Serotonin transporter gene variation is associated with alcohol sensitivity in rhesus macaques exposed to early-life stress. *Alcohol.: Clin. Exp. Res. 27*, 812–817.

50. Champoux, M., Bennett, A., Shannon, C., Higley, J. D., Lesch, K. P., and Suomi, S. J. (2002) Serotonin transporter gene polymorphism, differential early rearing, and behavior in rhesus monkey neonates. *Mol. Psychiatry 7*, 1058–1063.

51. Barr, C. S., Newman, T. K., Shannon, C., Parker, C., Dvoskin, R. L., Becker, M. L., Schwandt, M., Champoux, M., Lesch, K. P., Goldman, D., Suomi, S. J., and Higley, J. D. (2004) Rearing condition and *rh5-HTTLPR* interact to influence limbic-hypothalamic-pituitary-adrenal axis response to stress in infant macaques. *Biol. Psychiatry 55*, 733–738.

52. Kalin, N. H., Shelton, S. E., Fox, A. S., Rogers, J., Oakes, T. R., and Davidson, R. J. (2008) The serotonin transporter genotype is associated with intermediate brain phenotypes that depend on the context of eliciting stressor. *Mol. Psychiatry 13*, 1021–1027.

53. Bennett, A. J., Lesch, K. P., Heils, A., Long, J. C., Lorenz, J. G., Shoaf, S. E., Champoux, M., Suomi, S. J., Linnoila, M. V., and Higley, J. D. (2002) Early experience and serotonin transporter gene variation interact to influence primate CNS function. *Mol. Psychiatry 7*, 118–122.

54. Murphy, D. L., and Lesch, K. P. (2008) Targeting the murine serotonin transporter: Insights into human neurobiology. *Nat. Rev. Neurosci. 9*, 85–96.

55. Park, J., Show, Y., Quaiserova, V., Galligan, J. J., Fink, G. D., and Swain, G. M. (2005) Diamond microelectrodes for use in biological environments. *J. Electroanal. Chem. 583*, 56–68.

56. Gerhardt, G. A., and Hoffman, A. F. (2001) Effects of recording media composition on the responses of Nafion-coated carbon fiber microelectrodes measured using high-speed chronoamperometry. *J. Neurosci. Methods 109*, 13–21.

57. Gerhardt, G. A., Oke, A. F., Nagy, G., Moghaddam, B., and Adams, R. N. (1984) Nafion-coated electrodes with high selectivity for CNS electrochemistry. *Brain Res. 290*, 390–395.

58. Brazell, M. P., Kasser, R. J., Renner, K. J., Feng, J., Moghaddam, B., and Adams, R. N. (1987) Electrocoating carbon fiber microelectrodes with Nafion improves selectivity for electroactive neurotransmitters. *J. Neurosci. Methods 22*, 167–172.

59. Strojek, J. W., Granger, M. C., and Swain, G. M. (1996) Enhanced signal-to-background ratios in voltammetric measurements made at diamond thin-film electrochemical interfaces. *Anal. Chem. 68*, 2031–2037.

60. Manica, D. P., Mitsumori, Y., and Ewing, A. G. (2003) Characterization of electrode fouling and surface regeneration for a platinum electrode on an electrophoresis microchip. *Anal. Chem. 75*, 4572–4577.

61. Wisniewski, N., and Reichert, M. (2000) Methods for reducing biosensor membrane biofouling. *Colloids Surf., B 18*, 197–219.

62. Kawagoe, K. T., Zimmerman, J. B., and Wightman, R. M. (1993) Principles of voltammetry and microelectrode surface states. *J. Neurosci. Methods 48*, 225–240.

63. Kristensen, E. W., Kuhr, W. G., and Wightman, R. M. (1987) Temporal characterization of perfluorinated ion exchange coated microvoltammetric electrodes for *in vivo* use. *Anal. Chem. 59*, 1752–1757.

64. Halpern, J. M., Xie, S., Sutton, G. P., Higashikubo, B. T., Chestek, C. A., Lu, H., Chiel, H. J., and Martin, H. B. (2006) Diamond electrodes for neurodynamic studies in *Aplysia californica*. *Diamond Relat. Mater. 15*, 183–187.

65. Rudnick, G. (2006) Serotonin transporters: Structure and function. *J. Membr. Biol. 213*, 101–110.

66. Zhou, M., Engel, K., and Wang, J. (2007) Evidence for significant contribution of a newly identified monoamine transporter (PMAT) to serotonin uptake in the human brain. *Biochem. Pharmacol. 73*, 147–154.

67. Amenta, F., Bronzetti, E., Cantalamessa, F., El-Assouad, D., Felici, L., Ricci, A., and Tayebati, S. K. (2001) Identification of dopamine plasma membrane and vesicular transporters in human peripheral blood lymphocytes. *J. Neuroimmunol. 117*, 133–142.

68. Habert, E., Graham, D., Tahraoui, L., Claustre, Y., and Langer, S. Z. (1985) Characterization of [^{3}H]paroxetine binding to rat cortical membranes. *Eur. J. Pharmacol. 118*, 107–114.

69. Anderson, G. M., Gutknecht, L., Cohen, D. J., Brailly-Tabard, S., Cohen, J. H., Ferrari, P., Roubertoux, P. L., and Tordjman, S. (2002) Serotonin transporter promoter variants in autism: Functional effects and relationship to platelet hyperserotonemia. *Mol. Psychiatry 7*, 831–836.

70. Greenberg, B. D., Tolliver, T. J., Huang, S. J., Li, Q., Bengel, D., and Murphy, D. L. (1999) Genetic variation in the serotonin transporter promoter region affects serotonin uptake in human blood platelets. *Am. J. Med. Genet. 88*, 83–87.

71. Nobile, M., Begni, B., Giorda, R., Frigerio, A., Marino, C., Molteni, M., Ferrarese, C., and Battaglia, M. (1999) Effects of serotonin transporter promoter genotype on platelet serotonin transporter functionality in depressed children and adolescents. *J. Am. Acad. Child Adolesc. Psychiatry 38*, 1396–1402.

72. Kaiser, R., Muller-Oerlinghausen, B., Filler, D., Tremblay, P. B., Berghofer, A., Roots, I., and Brockmoller, J. (2002) Correlation between serotonin uptake in human blood platelets with the 44-bp polymorphism and the 17-bp variable number of tandem repeat of the serotonin transporter. *Am. J. Med. Genet. 114*, 323–328.

DOI: 10.1021/cn900012y | *ACS Chem. Neurosci.* (2010), *1*, 49–64

73. Patkar, A. A., Berrettini, W. H., Mannelli, P., Gopalakrishnan, R., Hoehe, M. R., Bilal, L., Weinstein, S., and Vergare, M. J. (2004) Relationship between serotonin transporter gene polymorphisms and platelet serotonin transporter sites among African-American cocaine-dependent individuals and healthy volunteers. *Psychiatr. Genet. 14*, 25–32.

74. Stoltenberg, S. F., Twitchell, G. R., Hanna, G. L., Cook, E. H., Fitzgerald, H. E., Zucker, R. A., and Little, K. Y. (2002) Serotonin transporter promoter polymorphism, peripheral indexes of serotonin function, and personality measures in families with alcoholism. *Am. J. Med. Genet. 114*, 230–234.

75. Naylor, L., Dean, B., Pereira, A., Mackinnon, A., Kouzmenko, A., and Copolov, D. (1998) No association between the serotonin transporter-linked promoter region polymorphism and either schizophrenia or density of the serotonin transporter in human hippocampus. *Mol. Med. 4*, 671–674.

76. Heinz, A., Jones, D. W., Mazzanti, C., Goldman, D., Ragan, P., Hommer, D., Linnoila, M., and Weinberger, D. R. (2000) A relationship between serotonin transporter genotype and *in vivo* protein expression and alcohol neurotoxicity. *Biol. Psychiatry 47*, 643–649.

77. van Dyck, C. H., Malison, R. T., Staley, J. K., Jacobsen, L. K., Seibyl, J. P., Laruelle, M., Baldwin, R. M., Innis, R. B., and Gelernter, J. (2004) Central serotonin transporter availability measured with [^{123}I]beta-CIT SPECT in relation to serotonin transporter genotype. *Am. J. Psychiatry 161*, 525–531.

78. Shioe, K., Ichimiya, T., Suhara, T., Takano, A., Sudo, Y., Yasuno, F., Hirano, M., Shinohara, M., Kagami, M., Okubo, Y., Nankai, M., and Kanba, S. (2003) No association between genotype of the promoter region of serotonin transporter gene and serotonin transporter binding in human brain measured by PET. *Synapse 48*, 184–188.

79. Willeit, M., Stastny, J., Pirker, W., Praschak-Rieder, N., Neumeister, A., Asenbaum, S., Tauscher, J., Fuchs, K., Sieghart, W., Hornik, K., Aschauer, H. N., Brucke, T., and Kasper, S. (2001) No evidence for *in vivo* regulation of midbrain serotonin transporter availability by serotonin transporter promoter gene polymorphism. *Biol. Psychiatry 50*, 8–12.

80. Heinz, A., Higley, J. D., Gorey, J. G., Saunders, R. C., Jones, D. W., Hommer, D., Zajicek, K., Suomi, S. J., Lesch, K. P., Weinberger, D. R., and Linnoila, M. (1998) *In vivo* association between alcohol intoxication, aggression, and serotonin transporter availability in nonhuman primates. *Am. J. Psychiatry 155*, 1023–1028.

81. Bengel, D., Jöhren, O., Andrews, A. M., Heils, A., Mössner, R., Sanvitto, G. L., Saavedra, J. M., Lesch, K.-P., and Murphy, D. L. (1997) Cellular localization and expression of the serotonin transporter in mouse brain. *Brain Res. 778*, 338–345.

82. Olivier, J. D., Van Der Hart, M. G., Van Swelm, R. P., Dederen, P. J., Homberg, J. R., Cremers, T., Deen, P. M., Cuppen, E., Cools, A. R., and Ellenbroek, B. A. (2008) A study in male and female 5-HT transporter knockout rats: an animal model for anxiety and depression disorders. *Neuroscience 152*, 573–584.

83. Holmes, A., Murphy, D. L., and Crawley, J. N. (2003) Abnormal behavioral phenotypes of serotonin transporter knockout mice: parallels with human anxiety and depression. *Biol. Psychiatry 54*, 953–959.

84. Mathews, T. A., Fedele, D. E., Coppelli, F. M., Avila, A. M., Murphy, D. L., and Andrews, A. M. (2004) Gene dose-dependent alterations in extraneuronal serotonin but not dopamine in mice with reduced serotonin transporter expression. *J. Neurosci. Methods 140*, 169–181.

85. Ansorge, M. S., Morelli, E., and Gingrich, J. A. (2008) Inhibition of serotonin but not norepinephrine transport during development produces delayed, persistent perturbations of emotional behaviors in mice. *J. Neurosci. 28*, 199–207.

86. Andersen, S. L., Dumont, N. L., and Teicher, M. H. (2002) Differences in behavior and monoamine laterality following neonatal clomipramine treatment. *Dev. Psychobiol. 41*, 50–57.

87. Popa, D., Lena, C., Alexandre, C., and Adrien, J. (2008) Lasting syndrome of depression produced by reduction in serotonin uptake during postnatal development: Evidence from sleep, stress, and behavior. *J. Neurosci. 28*, 3546–3554.

88. Sibille, E., and Lewis, D. A. (2006) SERT-ainly involved in depression, but when? *Am. J. Psychiatry 163*, 8–11.

89. Suzuki, A., Ivandini, T. A., Yoshimi, K., Fujishima, A., Oyama, G., Nakazato, T., Hattori, N., Kitazawa, S., and Einaga, Y. (2007) Fabrication, characterization, and application of boron-doped diamond microelectrodes for *in vivo* dopamine detection. *Anal. Chem. 79*, 8608–8615.

90. Granger, M. C., Witek, M., Xu, J., Wang, J., Hupert, M., Hanks, A., Koppang, M. D., Butler, J. E., Lucazeau, G., Mermoux, M., Strojek, J. W., and Swain, G. M. (2000) Standard electrochemical behavior of high-quality, boron-doped polycrystalline diamond thin-film electrodes. *Anal. Chem. 72*, 3793–3804.

91. Popa, E., Notsu, H., Miwa, T., Tryk, D. A., and Fujishima, A. (1999) Selective electrochemical detection of dopamine in the presence of ascorbic acid at anodized diamond thin film electrodes. *Electrochem. Solid-State Lett. 2*, 49–51.

92. Weng, J., Xue, J. M., Wang, J., Ye, J. S., Cui, H. F., Sheu, F. S., and Zhang, Q. Q. (2005) Gold-cluster sensors formed electrochemically at boron-doped-diamond electrodes: Detection of dopamine in the presence of ascorbic acid and thiols. *Adv. Funct. Mater. 15*, 639–647.

93. Shang, F., Zhou, L., Mahmoud, K. A., Hrapovic, S., Liu, Y., Moynihan, H. A., Glennon, J. D., and Luong, J. H. (2009) Selective nanomolar detection of dopamine using a boron-doped diamond electrode modified with an electropolymerized sulfobutylether-beta-cyclodextrin-doped poly(*N*-acetyltyramine) and polypyrrole composite film. *Anal. Chem. 81*, 4089–4098.

94. Park, S. G., Park, J. E., Cho, E. I., Hwang, J. H., and Ohsaka, T. (2006) Electrochemical detection of ascorbic acid and serotonin at a boron-doped diamond electrode modified with poly(N,N-dimethylaniline). *Res. Chem. Intermediat 32*, 595–601.

95. Luthman, J., Friedemann, M. N., Hoffer, B. J., and Gerhardt, G. A. (1997) *In vivo* electrochemical measurements

DOI: 10.1021/cn900012y | *ACS Chem. Neurosci.* (2010), *1*, 49–64

of serotonin clearance in rat striatum: Effects of neonatal 6-hydroxydopamine-induced serotonin hyperinnervation and serotonin uptake inhibitors. *J. Neural Transm. 104*, 379–397.

96. Sabeti, J., Adams, C. E., Burmeister, J., Gerhardt, G. A., and Zahniser, N. R. (2002) Kinetic analysis of striatal clearance of exogenous dopamine recorded by chronoamperometry in freely-moving rats. *J. Neurosci. Methods 121*, 41–52.

97. Gelernter, J., Kranzler, H., and Cubells, J. F. (1997) Serotonin transporter protein (*SLC6A4*) allele and haplotype frequencies and linkage disequilibria in African- and European-American and Japanese populations and in alcohol-dependent subjects. *Hum. Genet. 101*, 243–246.

DOI: 10.1021/cn900012y | *ACS Chem. Neurosci.* (2010), *1*, 49–64